Chemosphere 222 (2019) 656–664

Contents lists available at ScienceDirect

Chemosphere

journal homepage: www.elsevier.com/locate/chemosphere

Changes in ecotoxicity of naphthalene and alkylated naphthalenes during photodegradation in water

Hyun-Joong Kang, Yerin Jung, Jung-Hwan Kwon*

Division of Environmental Science and Ecological Engineering, Korea University, 145 Anam-ro, Seongbuk-gu, Seoul 02841, Republic of Korea

HIGHLIGHTS

- Toxicity changes of Naph and alkyl-Naph by photodegradation were studied.
- The observed photodegradation was well-explained by pseudo-first-order kinetics.
- The observed toxicity of Naph and alkyl-Naph was decreased by photodegradation.
- The toxic contribution by photodegradation products was significant.
- The identified photodegradation products were mainly oxygenated forms.

GRAPHICAL ABSTRACT

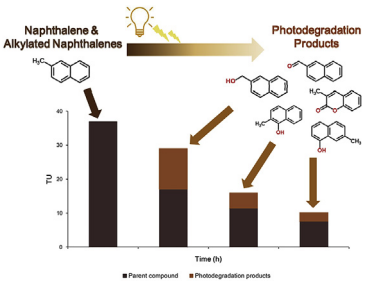

ARTICLE INFO

Article history:
Received 27 September 2018
Received in revised form
26 December 2018
Accepted 25 January 2019
Available online 29 January 2019

Handling Editor: Keith Maruya

Keywords:
Alkylated naphthalenes
Photodegradation
Oil spill
Photodegradation products
Mixture toxicity

ABSTRACT

Crude oil released into the environment contains many polycyclic aromatic hydrocarbons (PAHs). Alkylated PAHs are more abundant than unsubstituted PAHs and their toxicity is also of serious concern. Among the various physical, chemical, and biological weathering processes of crude oils, photodegradation is one of the most important for determining the environmental fate of oil residues. In this study, the photodegradation rate constants of naphthalene and alkylated naphthalenes were determined under simulated laboratory conditions at different temperature. Changes in the luminescence inhibition of *Aliivibrio fischeri*, as an indicator of the baseline toxicity, were observed in photodegradation mixtures. The major transformation products were also identified by gas chromatography–mass spectrometry. The photodegradation of naphthalene and the eight alkylated naphthalenes was described well by pseudo-first-order kinetics regardless of experimental temperature. The measured toxicity of the reaction mixtures obtained by photodegradative weathering slightly increased initially and then decreased with further weathering. In all cases, the observed toxicity was greater than accounted for by the parent compounds, indicating that the photodegradation products also contributed significantly to the overall toxicity of the mixtures. The identified photodegradation products were mostly oxygenated compounds such as alcohols, aldehydes, ketones, and quinones, which warrant further investigation.

1. Introduction

Marine oil spills, one of the most serious types of environmental disasters, have negative and long-term effects on marine environments. From 1907 to 2014, more than 7 million tons of crude oil was

* Corresponding author.
E-mail address: junghwankwon@korea.ac.kr (J.-H. Kwon).

https://doi.org/10.1016/j.chemosphere.2019.01.153
0045-6535/

released into the environment from more than 140 large spills (Li et al., 2016). The adverse ecological effects of these oil spill accidents have been studied for decades (Peterson et al., 2013; Bejarano and Michel, 2010; Diercks et al., 2010; Jiang et al., 2012).

Crude oils are made up of hundreds of major constituents and thousands of minor ones. Each crude oil has certain unique properties (Fingas, 2013). These properties influence how the spilled oil behaves and determine the fate and effects of the spilled oil in the environment (Fingas, 2013). Among the components of crude oil, polycyclic aromatic hydrocarbons (PAHs) are considered very important after oil spill accidents because they are toxic, mutagenic, carcinogenic, and relatively persistent in the environment (Jiang et al., 2012; Kang et al., 2014; Bellas et al., 2013). The levels of PAHs in oil-contaminated areas are commonly used to assess the degree of contamination and environmental recovery after oil spill accidents (Incardona et al., 2011; Di Toro et al., 2007; Loibner et al., 2004; Botello et al., 2015). Despite the presence of various forms of PAHs in crude oil, many studies have focused on 16 PAHs designated as priority pollutants by the U.S. Environmental Protection Agency (U.S. EPA) (Loibner et al., 2004; Botello et al., 2015; ATSDR, 1995; Redman et al., 2012; Jiang et al., 2010). However, chemical analyses of crude oils and petroleum products have revealed that the amount of alkylated PAHs is greater than that of unsubstituted PAHs (Pampanin and Sydnes, 2013; Yim et al., 2011; Neff et al., 2011). In particular, the alkylated homologues of naphthalene, phenanthrene, dibenzothiophene, fluorene, and chrysene were found to be present in crude oil at higher concentrations than the parent PAHs (Yang et al., 2015a). Furthermore, recent monitoring studies at various oil-contaminated sites have shown that the concentrations of alkylated PAHs are higher than those of the parent PAHs (Hawthorne et al., 2006; Liu et al., 2012; Tronczyński et al., 2004; Lee et al., 2013a). Our earlier study on the toxicity of Iranian heavy crude oil using the luminescence inhibition of *Aliivibrio fischeri* as an indicator for baseline toxicity revealed that the contribution of alkylated PAHs to the overall toxicity is approximately 10 times greater than that of the 16 PAHs identified by the U.S. EPA and that alkylated naphthalenes are the most important PAHs (Kang et al., 2014). For these reasons, alkylated PAHs are receiving increasing attention and their physico-chemical properties and toxicities have been evaluated (Andersson and Achten, 2015; Kang et al., 2016; Mu et al., 2014; Turcotte et al., 2011; Rhodes et al., 2005; Hong et al., 2012).

After an oil spill, the physical and chemical properties of crude oil undergo immediate changes that in combination are termed "weathering" (Fingas, 2013), including spreading, evaporation, dispersion, emulsification, dissolution, photooxidation, sedimentation, and biodegradation. These simultaneously occurring processes are complex (Mishra and Kumar, 2015) and may significantly change the physico-chemical properties and the composition of spilled oils. In particular, from a long-term perspective, photodegradation is a very important process leading to the chemical transformation of spilled oils (Genuino et al., 2012; King et al., 2014; Saeed et al., 2011; Wang et al., 2014; Ward et al., 2018; Yang et al., 2015b). As photodegradation progresses, the influence of spilled oil on the surrounding environment also changes owing to degradation of oil components such as PAHs (Cai et al., 2017; Fu et al., 2017). Although there are many studies on the photodegradation of PAHs in aquatic and soil environments, information is lacking on the photodegradation of alkylated PAHs and the toxicity of their photodegradation products.

In this study, the aqueous photodegradation of naphthalene and alkylated naphthalenes (1-methylnaphthalene, 2-methylnaphthalene, 1,2-dimethylnaphthalene, 1-ethylnaphthalene, 2-ethylnaphthalene, 1,4,5-trimethylnaphthalene, 2,3,5-trimethylnaphthalene, and 2,4,5-trimethylnaphthalene) which play an important role in the toxicity of crude oil was studied. The specific objectives were: 1) to determine the rates of photodegradation under simulated solar irradiation at 20, 25, 30, and 40 °C; 2) to evaluate the changes in the toxicity of the reaction mixtures with photodegradation using the luminescence inhibition of *A. fischeri* as a baseline toxicity marker; and 3) to identify the photodegradation products under simulated solar irradiation using gas chromatography–mass spectrometry (GC-MS).

2. Experimental

2.1. Materials

GC-grade 1,2-dimethylnaphthalene (96%), 1,4,5-trimethylnaphthalene (95%), 2,3,5-trimethylnaphthalene (95%), and 2,4,5-trimethylnaphthalene (98%) were purchased from Tokyo Chemical Industry Co. (Tokyo, Japan). Naphthalene (99%), 1-methylnaphthalene (95%), 2-methylnaphthalene (97%), 1-ethylnaphthalene (97%), and 2-ethylnaphthalene (99%) were purchased from Sigma-Aldrich (St Louis, MO, USA). Acetonitrile and acetone (HPLC ultra gradient solvent) were purchased from Avantor Performance Materials Inc. (Center Valley, PA, USA). Dichloromethane (DCM) was purchased from Daejung Chemical & Metals Co. (Siheung, Republic of Korea).

2.2. Photodegradation experiments

An incubator with a 250 W metal halide lamp (MSD 250/2 30H; Philips Lighting, Brussels, Belgium) was used for all photodegradation experiments. The emission spectrum of the metal halide lamp provides a good simulation of terrestrial solar radiation in the UV region above 300 nm (Shankar et al., 2015) and earlier studies used it as a light source for simulating sunlight (Marzooghi et al., 2018; Chen et al., 2007; Nudelman and Cabrera, 2002; Zhang et al., 2008). An incubator was used to maintain a constant temperature of 20, 25, 30, and 40 °C by cooling air. The water temperature was directly measured to ensure the photodegradation reactions occurs at desired temperature. The distance between the lamp and the aqueous samples that were stored in borosilicate vials (40 mL solution of naphthalene or alkylated naphthalenes) was 18 cm (Fig. 1). The UV irradiation of the metal halide lamp under the experimental conditions was measured at the beginning of the experiment using a portable UVX radiometer equipped with UVX-36 sensor covering 300–400 nm and calibrated at 365 nm

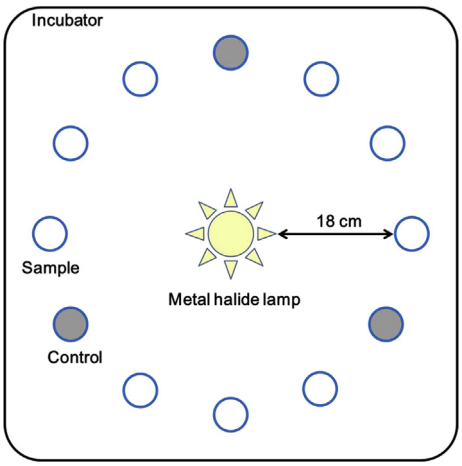

Fig. 1. Schematic diagram of the experimental apparatus used for the photodegradation tests.

(UltraViolet Products Ltd., San Gabriel, CA, USA) and the measured UV irradiation intensity was 62.1 W m^{-2}, which corresponds to the photon flux of 190 μmol m^{-2} s^{-1} at 365 nm. The initial concentrations were 12 mg L^{-1} for naphthalene, 1-methylnaphthalene, and 2-methylnaphthalene; 8 mg L^{-1} for 1-methylnaphthalene, 2-methylnaphthalene, and 1,2-dimethylnaphthalene; and 0.8 mg L^{-1} for 1,4,5-trimethylnaphthalene, 2,3,5-trimethylnaphthalene, and 2,4,5-trimethylnaphthalene. The solutions were prepared by dissolving crystals directly in deionized water below their water solubilities (Table S1, Supplementary Data). The photodegradation experiments were conducted for 6 h. All samples were run in triplicate with one negative control. The control was covered with aluminum foil to avoid irradiation. Sample aliquots (1 mL) were taken at predetermined time points (0, 1, 2, 4, and 6 h) and immediately mixed with acetonitrile (1 mL) to stop any further transformations. The solution was then subjected to ultra-high-performance liquid chromatography (UPLC) analysis. The total organic carbon (TOC) contents of the photodegraded samples were analyzed using a TOC analyzer (TOC-V CPH, Shimadzu, Kyoto, Japan). The reaction mixtures obtained after photodegradation of naphthalene and the alkylated naphthalenes for 6 h at 40 °C were subjected to liquid–liquid extraction for identification of the photodegradation products. A sample of 1000 mL prepared by pooling the initial or photodegraded samples was extracted three times using 50 mL of DCM–acetone (6:4, v/v). The DCM–acetone extract was then evaporated using a rotary evaporator and finally concentrated to 2 mL for analysis of the photodegradation products using GC-MS.

2.2.1. Photodegradation kinetics

The photodegradation of PAHs such as naphthalene in water can be described by pseudo-first-order kinetics (Chen et al., 1996; Jing et al., 2014; Kwon et al., 2009; Shemer and Linden, 2007; Wu and Shao, 2017), as represented by Eq. (1):

$$\ln\frac{C_t}{C_0} = -kt \tag{1}$$

where C_0 and C_t represent the concentrations at time zero and t, respectively, and k is the pseudo-first-order photodegradation rate constant, determined by linear regression of ln (C_t/C_0) vs. t.

2.3. Luminescence inhibition of A. fischeri

Changes in the acute toxicity of naphthalene and the eight alkylated naphthalenes during the photodegradation experiments at 40 °C were assessed by the luminescence inhibition by *A. fischeri* (strain NRRL B-11177) using a Microtox® M500 analyzer (Modern Water Inc., New Castle, DE, USA). Freeze-dried *A. fischeri* and diluent were purchased from Modern Water Inc. The photodegradation samples taken from the reaction mixtures of naphthalene and the eight alkylated naphthalenes at 0, 2, 4, and 6 h were directly applied to the bioassay. Luminescence inhibition after 15 min of exposure was determined according to the manufacturer's protocol. Negative controls prepared from deionized water and diluent did not show any statistically significant inhibition ($p = 0.05$). The effective dose for 50% inhibition (ED_{50}) values were derived using the Microtox Omni 4.2 software (Modern Water Inc.). To assess the toxicity changes during photodegradation of the alkylated naphthalenes, the test results were expressed in toxic units (*TU*).

For evaluating the overall effects of toxicants using the concentration-addition model, it is useful to express the toxicity of a chemical component using the concept of *TU* (Kang et al., 2014; Schmidt et al., 2013). The overall *TU* was calculated using the measured median effective dilution (ED_{50}) values (%) by:

$$\text{Overall } TU = \frac{100}{ED_{50}(\%)} = TU_{\text{parent chemical}} + TU_{\text{photodegradation products}} \tag{2}$$

The overall toxicity can also be calculated as the sum of the contributions of the individual parent chemicals and the photodegradation products. The *TU* of individual alkylated naphthalenes was calculated using the chemical analysis results for each photodegradation sample (Eq. (3)).

$$TU_{\text{parent chemical}} = \frac{\text{Remaining concentration of parent chemical in photodegradation sample } (\text{mg L}^{-1})}{EC_{50,\ \text{parent chemical}}(\text{mg L}^{-1})} \tag{3}$$

2.4. Instrumental analyses

The concentrations of naphthalene and the alkylated naphthalenes in aqueous samples were quantified using a Waters Acquity UPLC system equipped with a fluorescence detector. The mobile phase in isocratic mode was 70% acetonitrile and 30% water (v/v). The mixtures were separated on a Waters BEH C18 column (2.1 × 50 mm, 1.7 μm particle size) at a flow rate of 0.3 mL min^{-1} and 35 °C. Naphthalene and the alkylated naphthalenes were detected using the fluorescence detector with excitation (λ_{ex}) and emission wavelengths (λ_{em}) of 260 and 352 nm, respectively. The external standards were used for quantification. Calibration curves for naphthalene and eight alkylated naphthalenes were prepared using five standard solutions covering the concentration range of 0–6 h solutions. The correlation coefficients (r^2) were all greater than 0.99. Quality control standards were injected in every four injections and the measured concentration did not deviate more than 10%. The range of concentration was measured for all analytes was greater than the concentration of the lowest standard and higher than instrumental detection limits.

The DCM–acetone extracts of the photodegradation samples were analyzed using an Agilent 7890A gas chromatograph coupled with a 5975C series mass spectrometer (GC-MS). A HP-5MS 5% phenyl methyl siloxane capillary column (30 m × 0.25 mm ID × 0.25 μm film thickness) was used with helium as the carrier gas at a flow rate of 0.9 mL min^{-1}. The sample injection volume was 2 μL, and the temperatures of the inlet and the detector were 250 °C and 280 °C, respectively. The oven temperature was held at 40 °C for 1 min, ramped from 70 °C to 280 °C at 10 °C min^{-1}, and then held at 280 °C for 6 min. The scan range was from 35 to 550 m/z. The NIST05 MS library was used for tentative identification of the photodegradation products. All library-matched species exhibited a degree of match greater than 75%.

3. Results and discussion

3.1. Photodegradation kinetics

Fig. 2 shows the concentration and TOC changes of naphthalene

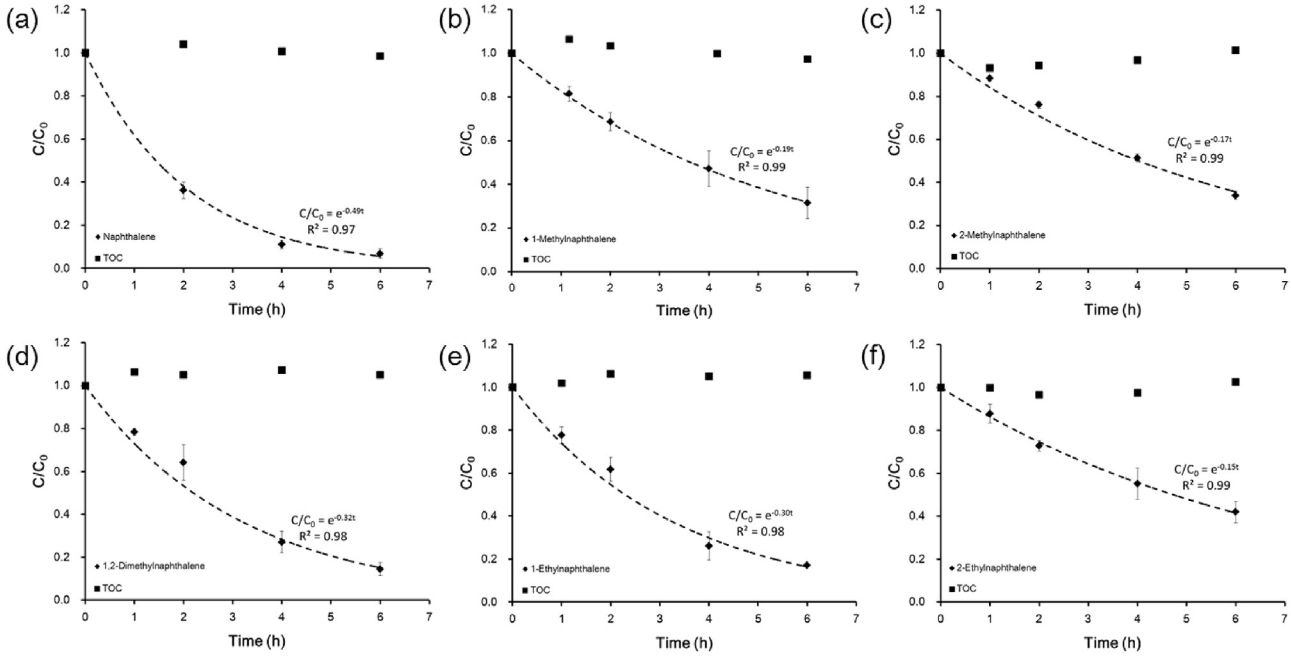

Fig. 2. Concentration and TOC changes of (a) naphthalene, (b) 1-methylnaphthalene, (c) 2-methylnaphthalene, (d) 1,2-dimethylnaphthalene, (e) 1-ethylnaphthalene, and (f) 2-ethylnaphthalene during photodegradation tests at 40 °C. Dashed lines describe the best fits using equation (1).

and various alkylated naphthalenes during the photodegradation tests at 40 °C. As shown, the concentrations of naphthalene and the alkylated naphthalenes decreased exponentially during the photodegradation tests, while the TOC concentration did not decrease much, indicating that naphthalene and the alkylated naphthalenes were not completely mineralized during the photodegradation tests. 1,4,5-Trimethylnaphthalene, 2,3,5-trimethylnaphthalene, and 2,4,5-trimethylnaphthalene were excluded from the TOC measurements because the initial concentrations of trimethylnaphthalenes were too low, owing to their limited water solubility, to be measured using a TOC analyzer.

The photodegradation of naphthalene and alkylated naphthalenes at all experimental temperature (20, 25, 30, and 40 °C) was fitted well by the pseudo-first-order kinetics (Fig. S1) and the obtained pseudo-first-order rate constants for the photodegradation (k) are listed in Table 1. The rate of photodegradation was accelerated as the temperature increased. For example, the measured photodegradation rate constant of naphthalene increased from 0.20 to 0.49 h^{-1} as the temperature rose from 20 to 40 °C.

The photodegradation rate constant of the alkylated naphthalenes at 40 °C was the highest for 1,4,5-trimethylnaphthalene, followed by 2,4,5-trimethylnaphthalene, naphthalene, 1,2-dimethylnaphthalene, 1-ethylnaphthalene, 2,3,5-trimethylnaphthalene, 1-methylnaphthalene, 2-methylnaphthalene, and 2-ethylnaphthalene.

The energy gaps between the highest occupied molecular orbital (HOMO) and the lowest unoccupied molecular orbital (LUMO) for naphthalene and the alkylated naphthalenes were calculated using ChemOffice Professional 15 (PerkinElmer Inc., San Jose, CA, USA) using the Molecular Orbital Package (MOPAC) program (MOPAC, 2012) and compared with the photodegradation rates. In several quantitative structure–activity relationship (QSAR) studies for predicting the photolysis of PAHs, the HOMO energy (E_{homo}), the LUMO energy (E_{lumo}), and the HOMO–LUMO energy gap ($E_{lumo} - E_{homo}$) have proven to be significant quantum chemical descriptors (Chen et al., 1996, 2001; Lu et al., 2005; Luo et al.,

Table 1
Molecular weights, octanol-water partition coefficients (K_{ow}), calculated highest occupied molecular orbital (HOMO)–lowest unoccupied molecular orbital (LUMO) energy gaps, photodegradation rate constants (k) at different temperatures from 20 to 40 °C, half-lives ($t_{1/2}$) obtained at 40 °C and calculated activation energy (E_a) using Arrhenius equation for naphthalene and the eight alkylated naphthalenes. Values of k and E_a represent mean ± standard deviation of triplicates.

Chemical	Molecular weight	log K_{ow} [a]	HOMO–LUMO gap (eV) [b]	k (h^{-1})				$t_{1/2}$ (h)	E_a (kJ mol^{-1})
				20 °C	25 °C	30 °C	40 °C		
Naphthalene	128	3.35	9.13	0.20 ± 0.01	0.27 ± 0.01	0.34 ± 0.01	0.49 ± 0.04	1.4	33 ± 5
1-Methylnaphthalene	142	3.72	9.01	0.087 ± 0.006	0.11 ± 0.01	0.13 ± 0.01	0.19 ± 0.04	3.6	29 ± 11
2-Methylnaphthalene	142	3.72	8.98	0.12 ± 0.01	0.14 ± 0.00	0.14 ± 0.00	0.17 ± 0.01	4.0	14 ± 1
1,2-Dimethylnaphthalene	156	4.26	8.81	0.18 ± 0.01	0.23 ± 0.01	0.28 ± 0.01	0.32 ± 0.03	2.2	21 ± 6
1-Ethylnaphthalene	156	4.21	9.02	0.15 ± 0.01	0.21 ± 0.04	0.21 ± 0.01	0.30 ± 0.02	2.3	25 ± 6
2-Ethylnaphthalene	156	4.21	8.96	0.072 ± 0.010	0.10 ± 0.01	0.12 ± 0.01	0.15 ± 0.01	4.7	25 ± 3
1,4,5-Trimethylnaphthalene	170	4.81	8.56	0.52 ± 0.01	0.53 ± 0.04	0.58 ± 0.05	0.69 ± 0.04	1.0	11 ± 3
2,3,5-Trimethylnaphthalene	170	4.81	8.90	0.15 ± 0.01	0.17 ± 0.01	0.18 ± 0.02	0.22 ± 0.04	3.1	16 ± 5
2,4,5-Trimethylnaphthalene	170	4.81	8.41	0.29 ± 0.04	0.35 ± 0.02	0.43 ± 0.07	0.56 ± 0.08	1.2	25 ± 2

[a] Predicted data using KOWWIN v1.68 in EPI Suite v4.1 (U.S. Environmental Protection Agency, 2012).
[b] Predicted data using ChemOffice Professional 15.

2015). However, as shown in Table 1, there are no apparent relationships between the HOMO–LUMO energy gaps and the measured rate constants in this study, likely because the HOMO–LUMO energy gaps of the selected compounds have a very narrow range of 8.41–9.13 eV, making it difficult to observe clear correlations with the photodegradation rate constants.

3.2. Determination of activation energies

As shown in Fig. 3, the observed photodegradation rates within the temperature range of 25–40 °C were explained by the Arrhenius equation:

$$\ln(k) = \frac{-E_a}{R}\frac{1}{T} + \ln(A) \quad (4)$$

where E_a is the activation energy (kJ mol^{-1}), R is the gas constant (J mol^{-1}K^{-1}), T is temperature (K), and A is the pre-exponential factor depending on compound. The activation energy (E_a) of this photodegradation process can also be determined by plotting the photodegradation rate constant versus temperature. The calculated activation energies of naphthalene and alkylated naphthalenes are listed in Table 1, ranging between 11 and 33 kJ mol^{-1}. Naphthalene has the highest activation energy of 33 kJ mol^{-1}. Higher activation energy represents higher sensitivity of the photodegradation rate to the environmental temperature (Jing et al., 2014). Using the measured activation energies (Table 1), for examples, photodegradation rate constants increase from 20 to 40 °C by 138, 75 and 33% for naphthalene, 1,2-dimethylnaphthalene and 1,4,5-trimethylnaphthalene, respectively.

3.3. Toxicity changes during photodegradation of naphthalene and alkylated naphthalenes

To evaluate the changes in toxicity caused by photodegradation, the naphthalene and alkylated naphthalene reaction mixtures were sampled after photodegradation for 0, 2, 4, and 6 h at 40 °C and used immediately for luminescence inhibition tests. The initial concentrations of 1,4,5-, 2,3,5-, and 2,4,5-trimethylnaphthalenes in the photodegradation experiments were lower than their water solubilities to ensure complete dissolution of crystals. It was difficult to observe luminescence inhibition that was significantly different from the negative control. This result is consistent with the short-term toxicity cutoff of trimethylnaphthalenes at approximately log K_{ow} of 5 with limited water solubility (Kang et al., 2016; Lee et al., 2013b). Table 2 shows the measured median effective concentration (EC_{50}) and ED_{50} values, as well as the calculated *TU*. The EC_{50} values obtained for naphthalene, 1-

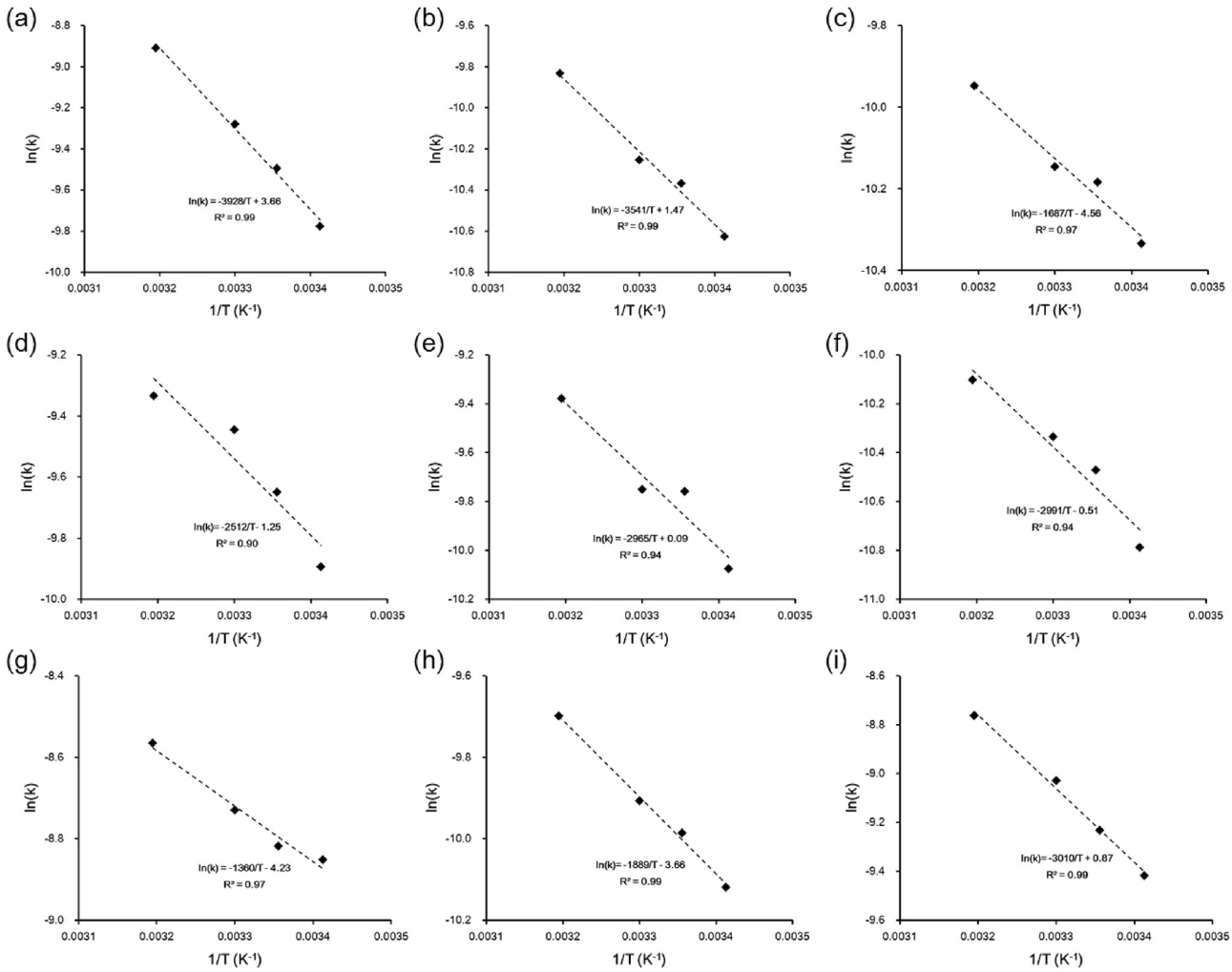

Fig. 3. Arrhenius plots for (a) naphthalene, (b) 1-methylnaphthalene, (c) 2-methylnaphthalene, (d) 1,2-dimethylnaphthalene, (e) 1-ethylnaphthalene, (f) 2-ethylnaphthalene, (g) 1,4,5-trimethylnaphthalene, (h) 2,3,5-trimethylnaphthalene and (i) 2,4,5-trimethylnaphthalene (T from 293 to 313 K).

Table 2
Octanol-water partition coefficients (K_{ow}), EC_{50} and ED_{50} values determined from the luminescence inhibition of *A. fischeri*, and calculated toxic units (*TU*) for naphthalene and the alkylated naphthalenes. Values in parentheses represent 95% confidence intervals.

Chemical	log K_{ow} [a]	EC_{50} (mg L^{-1})		ED_{50} (%)				*TU*			
		This study	Literature [b]	0 h	2 h	4 h	6 h	0 h	2 h	4 h	6 h
Naphthalene	3.35	0.52 (0.41, 0.66)	0.53	4.3 (3.4, 5.5)	3.6 (3.0, 4.3)	5.0 (4.1, 6.2)	6.1 (5.5, 8.2)	23	28	20	16
1-Methylnaphthalene	3.72	0.37 (0.34, 0.40)	0.50	3.1 (2.8, 3.3)	2.9 (2.7, 3.2)	3.8 (3.5, 4.2)	4.6 (4.1, 5.2)	33	34	26	22
2-Methylnaphthalene	3.72	0.32 (0.30, 0.35)	0.37	2.7 (2.5, 2.9)	3.4 (2.9, 4.0)	6.3 (5.7, 6.9)	9.8 (8.7, 11.1)	37	29	16	10
1,2-Dimethylnaphthalene	4.26	0.79 (0.67, 0.92)	–	9.8 (8.4, 11.5)	11.0 (10.3, 11.8)	16.1 (12.5, 20.8)	23.1 (13.6, 39.2)	10	9.1	6.2	4.3
1-Ethylnaphthalene	4.21	0.14 (0.14, 0.14)	0.18	1.8 (1.7, 1.8)	3.0 (2.8, 3.3)	4.6 (4.2, 5.1)	8.2 (7.3, 9.2)	57	33	22	12
2-Ethylnaphthalene	4.21	0.11 (0.10, 0.11)	0.09	2.0 (1.8, 2.2)	1.9 (1.7, 2.0)	2.9 (2.7, 3.1)	6.0 (5.5, 6.6)	51	54	35	17

[a] Predicted data using KOWWIN v1.68 in EPI Suite v4.1.
[b] Lee et al. (2013b).

methylnaphthalene, 2-methylnaphthalene, 1-ethylnaphthalene, and 2-ethylnaphthalene are 0.52, 0.37, 0.32, 0.14, and 0.16 mg L^{-1}, respectively, which are in good agreement with previously reported values (Lee et al., 2013b). For example, the previously reported values for 2-methylnaphthalene and 2-ethylnaphthalene are 0.37 and 0.09 mg L^{-1}, respectively (Lee et al., 2013b). These values are within a factor of 2 of the values determined in this study. The ED_{50} values of the photodegradation samples showed slight decreases for naphthalene, 1-methylnaphthalene, and 2-ethylnaphthalene after photodegradation for 2 h although they were not statistically significant ($p = 0.05$). With the exception of these initial decreases in ED_{50}, the observed ED_{50} values showed an increasing tendency with photodegradation time. For example, the ED_{50} values of naphthalene measured at 0 and 6 h increased from 4.3% to 6.1%.

Fig. 4 shows the *TU* changes of the reaction mixtures from photodegradation of naphthalene and the alkylated naphthalenes, with the contribution of the parent compounds estimated from their remaining concentrations. The overall toxicity of naphthalene and the alkylated naphthalenes tends to decrease during photodegradation. In the case of naphthalene and 2-ethylnaphthalene, the calculated initial *TU* values of 23 and 51, respectively, decreased to 13 and 17, respectively, after photodegradation for 6 h. In all the photodegradation samples, there were notable disparities between the observed *TU* value and that estimated from the measured concentration of the parent compound, indicating that the transformation products contribute a significant portion of the toxicity. This contribution of the photodegradation products to the toxicity was largest for naphthalene and smallest for 1-ethylnaphthalene. The contribution of the transformation products of naphthalene and alkylated naphthalenes to the overall toxicity generally increased as photodegradation proceeded, except in the case of 2-methylnaphthalene and 2-ethylnaphthalene. For example, the contributions of the phototransformation products of naphthalene to the overall toxicity were 27%, 39%, and 47% after 2, 4, and 6 h, respectively. These observations agree with earlier studies on the photodegradation products of PAHs that aqueous photodegradation produced oxygenated PAHs (Fasnacht and Blough, 2002, 2003) and toxicity of oxygenated PAHs could be comparable with that of PAHs

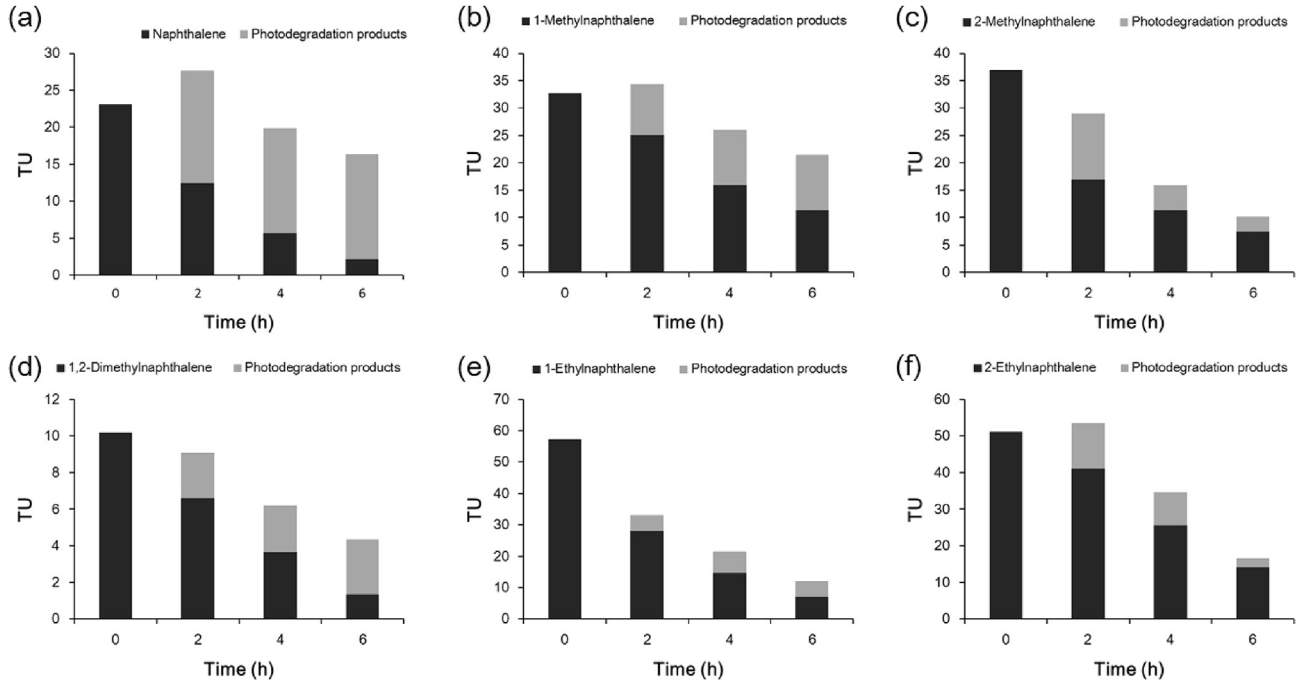

Fig. 4. Calculated *TU* changes for (a) naphthalene, (b) 1-methylnaphthalene, (c) 2-methylnaphthalene, (d) 1,2-dimethylnaphthalene, (e) 1-ethylnaphthalene, and (f) 2-ethylnaphthalene during photodegradation experiments.

(Lundstedt et al., 2007, 2014). Although luminescence inhibition of *A. fischeri* has been widely used as a baseline toxicity marker in many studies (Escher et al., 2017; Kang et al., 2014, 2016) for its simplicity, single toxicity tests are not sufficient to evaluate toxic potential of naphthalene and alkylated naphthalenes and their phototransformation products. Battery of multiple toxicity assays should be applied to evaluate their toxic potencies quantitatively.

Representative byproducts from the photooxidation of parent PAHs are oxygenated polycyclic aromatic hydrocarbons (oxy-PAHs). Thus, the major phototransformation products in this study were also likely oxygenated naphthalene and alkylated naphthalenes, which contribute to the observed overall toxicity. Owing to higher water solubility than that of their parents, oxy-PAHs are more environmentally mobile, but they are still persistent and toxic (Lundstedt et al., 2007; Layshock et al., 2010; Shen et al., 2011; Knecht et al., 2013; Salvo et al., 2016). Thus, oxy-PAHs are important co-contaminants that should be taken into account during the risk assessment of sites contaminated with high levels of PAHs (Lundstedt et al., 2007).

3.4. Identification of photodegradation products

To identify the photodegradation products of naphthalene and the alkylated naphthalenes, the obtained solvent extracts were analyzed by GC-MS. The mass spectral characteristics and molecular information identified by GC-MS of the parent compounds and their photodegradation products are summarized in Table 3 and Figs. S2–S8 (Supplementary Material). In the control samples covered with aluminum foil, the initial concentration of the parent compound did not change and no transformation products of naphthalene and the alkylated naphthalene were identified. As listed, the phototransformation products were mainly identified as alcohols, aldehydes, ketones, and quinones. It warrants further studies to identify more polar transformation products such as carboxylic acids because liquid-liquid extraction without derivatization reaction in this study is not suitable for extracting those compounds from aqueous solution.

Previous studies on the photodegradation process of PAHs have shown that photodegradation reactions are usually initiated by

Table 3
Information about the photodegradation products produced during photodegradation of naphthalene and the alkylated naphthalenes, as identified by GC-MS.

No.	Retention time (min)	Diagnostic mass fragments	Name	Empirical formula	Molecular weight	Matching quality (%)
(a)						
1	7.941	128, 102	Naphthalene (parent compound)	$C_{10}H_8$	128	95
2	8.598	105, 77.1, 134	Phthalaldehyde	$C_8H_6O_2$	134	87
3	9.113	132.1, 104.1, 78.1	1-Indanone	C_9H_8O	132	97
4	9.520	104, 76, 148	2-Benzofuran-1,3-dione	$C_8H_4O_3$	148	86
5	10.069	105.1, 134, 77.1	2-Benzofuran-1(3*H*)-one	$C_8H_6O_2$	134	91
6	10.904	158, 104, 130	1,4-Naphthoquinone	$C_{10}H_6O$	158	90
7	11.213	146, 118, 89.1	2*H*-Chromen-2-one	$C_9H_6O_2$	146	91
8	12.009	44.1, 115.1, 144.1	1-Naphthol	$C_{10}H_8O$	144	95
(b)						
1	9.812	142.2, 115.1	1-Methylnaphthalene (parent compound)	$C_{11}H_{10}$	142	90
2	10.023	105, 134, 77.1	2-Benzofuran-1(3*H*)-one	$C_8H_6O_2$	134	91
3	10.304	105.1, 133, 148.1	1-(3,4-Dimethylphenyl)ethanone	$C_{10}H_{12}O$	148	87
4	10.904	119, 148.1, 91.1	7-Methyl-1-benzofuran-3(2*H*)-one	$C_9H_8O_2$	148	80
5	11.213	146, 118, 89.1	2*H*-Chromen-2-one	$C_9H_6O_2$	146	91
6	11.517	119.1, 148, 91.1	6-Methyl-2-benzofuran-1(3*H*)-one	$C_9H_8O_2$	148	86
7	11.980	156.1, 128.1	1-Naphthaldehyde	$C_{11}H_8O$	156	98
8	12.632	129.1, 158.1	1-Naphthylmethanol	$C_{11}H_{10}O$	158	94
(c)						
1	9.560	141.2, 115.1	2-Methylnaphthalene (parent compound)	$C_{11}H_{10}$	142	94
2	10.035	105, 134, 77.1	2-Benzofuran-1(3*H*)-one	$C_8H_6O_2$	134	91
3	11.030	158.1, 115, 129.1	7-Methyl-1-naphthol	$C_{11}H_{10}O$	158	78
4	11.482	119.1, 148, 91.1	4-Methyl-2-benzofuran-1(3*H*)-one	$C_9H_8O_2$	148	86
5	11.648	119.1, 148, 91.1	4-Methylphthalaldehyde	$C_9H_8O_2$	148	95
6	11.917	131.1, 160	3-Methyl-2*H*-chromen-2-one	$C_{10}H_8O_2$	160	94
7	12.015	156.1, 127.1	2-Naphthaldehyde	$C_{11}H_8O$	156	97
8	12.455	160, 132, 104.1	7-Methyl-2*H*-chromen-2-one	$C_{10}H_8O_2$	160	94
9	12.507	158.1, 129.1, 115.1	2-Methyl-1-naphthol	$C_{11}H_{10}O$	158	89
10	12.690	29.1, 158.1, 141.1	2-Naphthylmethanol	$C_{11}H_{10}O$	158	94
11	13.033	188, 131, 105	2-Hydroxy-3-methyl-1,4-naphthoquinone	$C_{11}H_8O_3$	188	94
(d)						
1	11.586	141.1, 156.1, 115.1	1,2-Dimethylnaphthalene (parent compound)	$C_{12}H_{12}$	156	94
2	10.251	105, 132.9, 147.9	1-(3,4-Dimethylphenyl)ethanone	$C_{10}H_{12}O$	148	87
3	12.416	133, 162, 105	6,7-Dimethyl-2-benzofuran-1(3*H*)-one	$C_{10}H_{10}O$	162	76
4	13.039	133, 162, 105	4,5-Dimethyl-2-benzofuran-1(3*H*)-one	$C_{10}H_{10}O$	162	91
5	13.113	170, 141, 115	8-Methyl-1-naphthaldehyde	$C_{12}H_{10}O$	170	80
(e)						
1	10.809	115, 141, 156	1-Ethylnaphthalene (parent compound)	$C_{12}H_{12}$	156	60
2	10.019	105, 77, 134	2-Benzofuran-1(3*H*)-one	$C_8H_6O_2$	134	97
3	11.221	118, 146, 89	2*H*-Chromen-2-one	$C_9H_6O_2$	146	93
4	11.763	119, 147, 162	2-Ethyl-1,4-benzodioxine	$C_{10}H_{10}O_2$	162	86
5	12.643	127, 155, 170	1-(2-Naphthyl)ethanone	$C_{12}H_{10}O$	170	95
6	12.871	129, 144, 157, 172	1-(2-Naphthyl)ethanol	$C_{12}H_{12}O$	172	95
7	14.075	171, 115, 186	1-(2-Hydroxy-1-naphthyl)ethanone	$C_{12}H_{10}O_2$	186	94
(f)						
1	10.882	141.2, 156.2, 115.1	2-Ethylnaphthalene (parent compound)	$C_{12}H_{12}$	156	83
2	12.879	129.1, 172.1, 157.1	1-(2-Naphthyl)ethanol	$C_{12}H_{12}O$	172	97
3	12.941	155.1, 127.1, 170.1	1-(2-Naphthyl)ethanone	$C_{12}H_{10}O$	170	95
4	13.113	157.1, 172.1, 129.1	3-Ethyl-1-naphthol	$C_{12}H_{12}O$	172	90

hydroxylation of PAHs, followed by a series of oxidation processes, to finally yield photodegradation products in the form of smaller molecules (Woo et al., 2009; Theurich et al., 1997). For naphthalene, the identified photodegradation products were consistent with those identified in a previous study (Woo et al., 2009), including 1,4-naphthoquinone, 2*H*-chromen-2-one, and 1-naphthol. For all the alkylated naphthalenes, except 1,2-dimethylnaphthalene, hydroxylated degradation products were identified. As an example, 1-naphthol, 1-naphthylmethanol, and 1-(2-naphthyl)ethanol were identified as photodegradation products of naphthalene, 1-methylnaphthalene, and 1-ethylnaphthalene, respectively. Various other oxygenated degradation products were also identified. These oxygenated products are suspected to contribute to the overall toxicity of the degradation mixtures in Section 3.2, but further studies are required to quantitatively evaluate their toxicity.

4. Conclusions

The present study focused on the photodegradation of naphthalene and selected alkylated naphthalenes and the changes in toxicity as phototransformation proceeds in aquatic environments. The observed decreases in the concentration of naphthalene and the eight alkylated naphthalenes were well explained by pseudo-first-order kinetics regardless of temperature with coefficients of determination (R^2) between 0.96 and 0.99. The photodegradation rates decreased in the order of 1,4,5-trimethylnaphthalene, 2,4,5-trimethylnaphthalene, naphthalene, 1,2-dimethylnaphthalene, 1-ethylnaphthalene, 2,3,5-trimethylnaphthalene, 1-methylnaphthalene, 2-methylnaphthalene, and 2-ethylnaphthalene. In general, the observed toxicity of the phototransformation mixtures from naphthalene and the alkylated naphthalenes decreased with the degree of photodegradation. The slight increases in toxicity observed after 2 h for naphthalene, 1-methylnaphthalene, and 1-ethylnaphthalene are likely due to the formation of more polar oxygenated transformation products with comparable toxic potencies. Thus, the photodegradation products from naphthalene and the alkylated naphthalenes, which are mainly oxygenated PAHs, are suspected to be important contributors to the overall toxicity of the reaction mixtures. Although several oxygenated PAHs were tentatively identified using GC-MS, further investigations on the quantitative analysis of transformation products of alkylated naphthalenes and their photodegradation pathways and toxicities are necessary.

Acknowledgment

This research was part of the project entitled “Oil Spill Environmental Impact Assessment and Environmental Restoration (PM57431)” funded by the Ministry of Oceans and Fisheries, Korea and supported by a Korea University Grant.

Appendix A. Supplementary data

Supplementary data to this article can be found online at https://doi.org/10.1016/j.chemosphere.2019.01.153.

References

Agency for toxic substances and disease registry (ATSDR), 1995. Toxicology Profile for Polycyclic Aromatic Hydrocarbons (PAHs). U.S department for health and human service, public health service, Atlanta.

Andersson, J.T., Achten, C., 2015. Time to sayg to the 16 EPA PAHs? Toward an up-to-date use of PACs for environmental purposes. Polycycl. Aromat. Comp. 35, 330–354.

Bejarano, A.C., Michel, J., 2010. Large-scale risk assessment of polycyclic aromatic hydrocarbons in shoreline sediments from Saudi Arabia: environmental legacy after twelve years of the Gulf war oil spill. Environ. Pollut. 158, 1561–1569.

Bellas, J., Saco-Alvarez, L., Nieto, O., Bayona, J.M., Albaiges, J., Beiras, R., 2013. Evaluation of artificially-weathered standard fuel oil toxicity by marine invertebrate embryogenesis bioassays. Chemosphere 90, 1103–1108.

Botello, A.V., Soto, L.A., Ponce-Vélez, G., Susana Villanueva, F., 2015. Baseline for PAHs and metals in NW Gulf of Mexico related to the Deepwater Horizon oil spill. Estuar. Coast. Shelf Sci. 156, 124–133.

Cai, Z., Liu, W., O'Reilly, S.E., Zhao, D., 2017. Effects of oil dispersants on photodegradation of parent and alkylated anthracene in seawater. Environ. Pollut. 229, 272–280.

Chen, J., Peijnenburg, W.J.G.M., Quan, X., Chen, S., Martens, D., Schramm, K.-W., Kettrup, A., 2001. Is it possible to develop a QSPR model for direct photolysis half-lives of PAHs under irradiation of sunlight? Environ. Pollut. 114, 137–143.

Chen, J.W., Kong, L.R., Zhum, C.M., Huang, Q.G., Wang, L.S., 1996. Correlation between photolysis rate constants of polycyclic aromatic hydrocarbons and frontier molecular orbital energy. Chemosphere 33, 1143–1150.

Chen, Y., Wu, F., Lin, Y., Deng, N., Bazhin, N., Glebov, E., 2007. Photodegradation of glyphosate in the ferrioxalate system. J. Hazard. Mater. 148, 360–365.

Di Toro, D.M., McGrath, J.A., Stubblefield, W.A., 2007. Predicting the toxicity of neat and weathered crude oil: toxic potential and the toxicity of saturated mixtures. Environ. Toxicol. Chem. 26, 24–36.

Diercks, A.R., Highsmith, R.C., Asper, V.L., Joung, D., Zhou, Z., Guo, L., Shiller, A.M., Joye, S.B., Teske, A.P., Guinasso, N., Wade, T.L., Lohrenz, S.E., 2010. Characterization of subsurface polycyclic aromatic hydrocarbons at the Deepwater Horizon site. Geophys. Res. Lett. 37, L20602.

Escher, B.I., Baumer, A., Bittermann, K., Henneberger, L., König, M., Kühnert, C., Klüver, N., 2017. General baseline toxicity QSAR for nonpolar, polar and ionisable chemicals and their mixtures in the bioluminescence inhibition assay with *Aliivibrio fischeri*. Environ. Sci. Process. Impacts 19, 414–428.

Fasnacht, M.P., Blough, N.V., 2002. Aqueous photodegradation of polycyclic aromatic hydrocarbons. Environ. Sci. Technol. 36, 4364–4369.

Fasnacht, M.P., Blough, N.V., 2003. Mechanisms of the aqueous photodegradation of polycyclic aromatic hydrocarbons. Environ. Sci. Technol. 37, 5767–5772.

Fingas, M., 2013. The Basics of Oil Spill Cleanup, third ed. CRC Press, Boca Raton, FL.

Fu, J., Gong, Y., Cai, Z., O'Reilly, S.E., Zhao, D., 2017. Mechanistic investigation into sunlight-facilitated photodegradation of pyrene in seawater with oil dispersants. Mar. Pollut. Bull. 114, 751–758.

Genuino, H.C., Horvath, D.T., King'ondu, C.K., Hoag, G.E., Collins, J.B., Suib, S.L., 2012. Effects of visible and UV light on the characteristics and properties of crude oil-in-water (O/W) emulsions. Photochem. Photobiol. Sci. 11, 692–702.

Hawthorne, S.B., Miller, D.J., Kreitinger, J.P., 2006. Measurement of total polycyclic aromatic hydrocarbon concentrations in sediments and toxic units used for estimating risk to benthic invertebrates at manufactured gas plant sites. Environ. Toxicol. Chem. 25, 287–296.

Hong, S., Khim, J.S., Ryu, J., Park, J., Song, S.J., Kwon, B.-O., Choi, K., Ji, K., Seo, J., Lee, S., Park, J., Lee, J., Choi, Y., Lee, K.T., Kim, C.-K., Shim, W.J., Naile, J.E., Giesy, J.P., 2012. Two years after the *Hebei Spirit* oil spill: residual crude-derived hydrocarbons and potential AhR-mediated activities in coastal sediments. Environ. Sci. Technol. 46, 1406–1414.

Incardona, J.P., Vines, C.A., Anulacion, B.F., Baldwin, D.H., Day, H.L., French, B.L., Labenia, J.S., Linbo, T.L., Myers, M.S., Olson, O.P., Sloan, C.A., Sol, S., Griffin, F.J., Menard, K., Morgan, S.G., West, J.E., Collier, T.K., Ylitalo, G.M., Cherr, G.N., Scholz, N.L., 2011. Unexpectedly high mortality in Pacific herring embryos exposed to the 2007 Cosco Busan oil spill in San Francisco Bay. Proc. Natl. Acad. Sci. U.S.A. 109, E51–E55.

Jiang, Z., Huang, Y., Xu, X., Liao, Y., Shou, L., Liu, J., Chen, Q., Zeng, J., 2010. Advance in the toxic effects of petroleum water accommodated fraction on marine plankton. Acta Ecol. Sin. 30, 8–15.

Jiang, Z.B., Huang, Y.J., Chen, Q.Z., Zeng, J.N., Xu, X.Q., 2012. Acute toxicity of crude oil water accommodated fraction on marine copepods: the relative importance of acclimatization temperature and body size. Mar. Environ. Res. 81, 12–17.

Jing, L., Chen, B., Zhang, B., Zheng, J., Liu, B., 2014. Naphthalene degradation in seawater by UV irradiation: the effects of fluence rate, salinity, temperature and initial concentration. Mar. Pollut. Bull. 81, 149–156.

Kang, H.-J., Lee, S.-Y., Kwon, J.-H., 2016. Physico-chemical properties and toxicity of alkylated polycyclic aromatic hydrocarbons. J. Hazard. Mater. 312, 200–207.

Kang, H.-J., Lee, S.-Y., Roh, J.-Y., Yim, U.H., Shim, W.J., Kwon, J.-H., 2014. Prediction of ecotoxicity of heavy crude oil: contribution of measured components. Environ. Sci. Technol. 48, 2962–2970.

King, S.M., Leaf, P.A., Olson, A.C., Ray, P.Z., Tarr, M.A., 2014. Photolytic and photocatalytic degradation of surface oil from the Deepwater Horizon spill. Chemosphere 95, 415–422.

Knecht, A.L., Goodale, B.C., Truong, L., Simonich, M.T., Swanson, A.J., Matzke, M.M., Anderson, K.A., Waters, K.M., Tanguay, R.L., 2013. Comparative developmental toxicity of environmentally relevant oxygenated PAHs. Toxicol. Appl. Pharmacol. 271, 266–275.

Kwon, S.H., Kim, J.H., Cho, D., 2009. An analysis method for degradation kinetics of lowly concentrated PAH solutions under UV light and ultrasonication. J. Ind. Eng. Chem. 15, 157–162.

Layshock, J., Wilson, G., Anderson, K.A., 2010. Ketone and quinone-substituted polycyclic aromatic hydrocarbons in mussel tissue, sediment, urban dust, and diesel particulate matrices. Environ. Toxicol. Chem. 29, 2450–2460.

Lee, C.-H., Lee, J.-H., Sung, C.-G., Moon, S.-D., Kang, S.-K., Lee, J.-H., Yim, U.H., Shim, W.J., Ha, S.Y., 2013a. Monitoring toxicity of polycyclic aromatic hydrocarbons in intertidal sediments for five years after the Hebei Spirit oil spill in Taean, Republic of Korea. Mar. Pollut. Bull. 76, 241–249.

Lee, S.-Y., Kang, H.-J., Kwon, J.-H., 2013b. Toxicity cutoff of aromatic hydrocarbons for luminescence inhibition of *Vibrio fischeri*. Ecotoxicol. Environ. Saf. 94, 116–122.
Li, P., Cai, Q., Lin, W., Chen, B., Zhang, B., 2016. Offshore oil spill response practices and emerging challenges. Mar. Pollut. Bull. 110, 6–27.
Liu, Z., Liu, J., Zhu, Q., Wu, W., 2012. The weathering of oil after the Deepwater Horizon oil spill: insights from the chemical composition of the oil from the sea surface, salt marshes and sediments. Environ. Res. Lett. 7, 035302.
Loibner, A.P., Szolar, O.H.J., Braun, R., Hirmann, D., 2004. Toxicity testing of 16 priority polycyclic aromatic hydrocarbons using LUMISTOX®. Environ. Toxicol. Chem. 23, 557–564.
Lu, G.-N., Dang, Z., Tao, X.-Q., 2005. QSPR study on direct photolysis half-lives of PAHs in water surface. J. Theor. Comput. Chem. 4, 811–822.
Lundstedt, S., Bandowe, B.A.M., Wilcke, W., Boll, E., Christensen, J.H., Vila, J., Grifoll, M., Faure, P., Biache, C., Lorgeoux, C., Larsson, M., Irgum, K.F., Ivarsson, P., Ricci, M., 2014. First intercomparison study on the analysis of oxygenated polycyclic aromatic hydrocarbons (oxy-PAHs) and nitrogen heterocyclic polycyclic aromatic compounds (N-PACs) in contaminated soil. Trends Anal. Chem. 57, 83–92.
Lundstedt, S., White, P.A., Lemieux, C.L., Lynes, K.D., Lambert, I.B., Öberg, L., Haglund, P., Tysklind, M., 2007. Sources, fate, and toxic hazards of oxygenated polycyclic aromatic hydrocarbons (PAHs) at PAH- contaminated sites. Ambio 36, 475–485.
Luo, Z.-H., Wei, C.-L., He, N.-N., Sun, Z.-G., Li, H.-X., Chen, D., 2015. Correlation between the photocatalytic degradability of PAHs over Pt/TiO_2-SiO_2 in water and their quantitative molecular structure. J. Nanomater. 284834.
Marzooghi, S., Finch, B.E., Stubblefield, W.E., Di Toro, D.M., 2018. Predicting phototoxicity of alkylated PAHs, mixtures of PAHs, and water accommodated fractions (WAF) of neat and weathered petroleum with the phototoxic target lipid model. Environ. Toxicol. Chem. 37, 2165–2174.
Mishra, A.K., Kumar, M.S., 2015. Weathering of oil spill: modeling and analysis. Aquat. Procedia 4, 435–442.
MOPAC, 2012. Available online from: http://openmopac.net/MOPAC2012.html.
Mu, J., Wang, J., Jin, F., Wang, X., Hong, H., 2014. Comparative embryotoxicity of phenanthrene and alkyl-phenanthrene to marine medaka (*Oryzias melastigma*). Mar. Pollut. Bull. 85, 505–515.
Neff, J., Lee, K., De Blois, E.M., 2011. Produced water: overview of composition, fate, and effects. In: Lee, K., Neff, J. (Eds.), Produced Water. Environmental Risks and Advances in Mitigation Technologies. Springer, New York, pp. 3–54.
Nudelman, N.S., Cabrera, C.G., 2002. Spectrofluorimetric assay for the photodegradation products of alprazolam. J. Pharmaceut. Biomed. Anal. 30, 887–893.
Pampanin, D.M., Sydnes, M.O., 2013. Polycyclic aromatic hydrocarbons a constituent of petroleum: presence and influence in the aquatic environment. In: Kutcherov, V. (Ed.), Hydrocarbon. InTech, Rijeka, pp. 83–118.
Peterson, C.H., Rice, S.D., Short, J.W., Esler, D., Bodkin, J.L., Ballachey, B.E., Irons, D.B., 2013. Long-term ecosystem response to the Exxon Valdez oil spill. Science 302, 2082–2086.
Redman, A.D., Parkerton, T.F., McGrath, J.A., Di Toro, D.M., 2012. Petrotox: an aquatic toxicity model for petroleum substances. Environ. Toxicol. Chem. 31, 2498–2506.
Rhodes, S., Farwell, A., Hewitt, L.M., MacKinnon, M., Dixon, D.G., 2005. The effects of dimethylated and alkylated polycyclic aromatic hydrocarbons on the embryonic development of the Japanese medaka. Ecotoxicol. Environ. Saf. 60, 247–258.
Saeed, T., Ali, L.N., Al-Bloushi, A., Al-Hashash, H., Al-Bahloul, M., Al-Khabbaz, A., Al-Khayat, A., 2011. Effect of environmental factors on photodegradation of polycyclic aromatic hydrocarbons (PAHs) in the water-soluble fraction of Kuwait crude oil in seawater. Mar. Environ. Res. 72, 143–150.
Salvo, L.M., Severino, D., Silva de Assis, H.C., da Silva, J.R.M.C., 2016. Photochemical degradation increases polycyclic aromatic hydrocarbon (PAH) toxicity to the grouper *Epinephelus marginatus* as assessed by multiple biomarkers. Chemosphere 144, 540–547.
Schmidt, S.N., Holmstrup, M., Smith, K.E.C., Mayer, P., 2013. Passive dosing of polycyclic aromatic hydrocarbon (PAH) mixtures to terrestrial springtails: linking mixture toxicity to chemical activities, equilibrium lipid concentrations, and toxic units. Environ. Sci. Technol. 47, 7020–7027.
Shankar, R., Shim, W.J., An, J.G., Yim, U.H., 2015. A practical review on photooxidation of crude oil: laboratory lamp setup and factors affecting it. Water Res. 68, 304–315.
Shemer, H., Linden, K.G., 2007. Aqueous photodegradation and toxicity of the polycyclic aromatic hydrocarbons fluorene, dibenzofuran and dibenzothiophene. Water Res. 41, 853–861.
Shen, G., Tao, S., Wang, W., Yang, Y., Ding, J., Xue, M., Min, Y., Zhu, C., Shen, H., Li, W., Wang, B., Wang, R., Wang, W., Wang, X., Russell, A.G., 2011. Emission of oxygenated polycyclic aromatic hydrocarbons from indoor solid fuel combustion. Environ. Sci. Technol. 45, 3459–3465.
Theurich, J., Bahnemann, D.W., Vogel, R., Ehamed, F.E., Alhakimi, G., Rajab, I., 1997. Photocatalytic degradation of naphthalene and anthracene: GC-MS analysis of the degradation pathway. Res. Chem. lntermed. 23, 247–274.
Tronczyński, J., Munschy, C., Héas-Moisan, K., Guiot, N., Truquet, I., Olivier, N., Men, S., Furaut, A., 2004. Contamination of the Bay of Biscay by polycyclic aromatic hydrocarbons (PAHs) following the T/V “Erika” oil spill. Aquat. Living Resour. 17, 243–259.
Turcotte, D., Akhtar, P., Bowerman, M., Kiparissis, Y., Brown, R.S., Hodson, P.V., 2011. Measuring the toxicity of alkyl-phenanthrenes to early life stages of medaka (*Oryzias latipes*) using partition-controlled delivery. Environ. Toxicol. Chem. 30, 487–495.
US Environmental Protection Agency, 2012. EPISuite v4.10.
Wang, C., Chen, B., Zhang, B., Guo, P., Zhao, M., 2014. Study of weathering effects on the distribution of aromatic steroid hydrocarbons in crude oils and oil residues. Environ. Sci.: Processes Impacts 16, 2408–2414.
Ward, C.P., Sharpless, C.M., Valentine, D.L., French-McCay, D.P., Aeppli, C., White, H.K., Rodgers, R.P., Gosselin, K.M., Nelson, R.K., Reddy, C.M., 2018. Partial photochemical oxidation was a dominant fate of Deepwater Horizon surface oil. Environ. Sci. Technol. 52, 1797–1805.
Woo, O.T., Chung, W.K., Chow, A.T., Wong, P.K., 2009. Photocatalytic oxidation of polycyclic aromatic hydrocarbons: intermediates identification and toxicity testing. J. Hazard. Mater. 168, 1192–1199.
Wu, S., Shao, Y., 2017. Study of kinetics mechanism of PAHs photodegradation in solution. Procedia Earth Planet. Sci. 17, 348–351.
Yang, C., Wang, Z., Hollebone, B.P., Brown, C.E., Yang, Z., Landriault, M., 2015a. Chromatographic fingerprinting analysis of crude oils and petroleum products. In: Fingas, M. (Ed.), Handbook of Oil Spill Science and Technology. Wiley, New Jersey, pp. 95–164.
Yang, Z., Hollebone, B.P., Wang, Z., Yang, C., Brown, C., Zhang, G., Landriault, M., Ruan, X., 2015b. A preliminary study for the photolysis behavior of biodiesel and its blends with petroleum oil in simulated freshwater. Fuel 139, 248–256.
Yim, U.H., Ha, S.Y., An, J.G., Won, J.H., Han, G.M., Hong, S.H., Kim, M., Jung, J.,-H., Shim, W.J., 2011. Fingerprint and weathering characteristics of stranded oils after the Hebei Spirit oil spill. J. Hazard. Mater. 197, 60–69.
Zhang, X., Wu, F., Wu, X.W., Chen, P., Deng, N., 2008. Photodegradation of acetaminophen in TiO_2 suspended solution. J. Hazard. Mater. 157, 300–307.